but not 1 mg/kg (Fig. 4, E and F). As expected (*21*), histologic examination of the kidneys of STx1-treated mice revealed extensive damage in the cortical convoluted tubules, whereas animals protected by Mn^{2+} showed no STx1-induced renal damage (Fig. 4G). Thus, Mn^{2+} effectively protects against STx-induced toxicity and death in vivo even during fulminant systemic toxicosis.

In conclusion, Mn^{2+} may be effective in the management of STx infections. In contrast to other experimental strategies (*20*, *23*–*25*), Mn^{2+} is an essential nutrient, its toxicology is well studied (*26*, *27*), and it is already approved for oral and intravenous use. The low cost and wide availability of Mn^{2+} make it amenable for use in developing countries, where >95% of STx infections occur. Further, it may be possible to combine Mn^{2+} with antibiotic therapy because Mn^{2+} may block the toxic effects of STx released from dying bacteria.

References and Notes

1. T. Ochoa, T. G. Cleary, in *Oski's Pediatrics: Principles and Practice*, J. A. McMillan *et al.*, Eds. (Lippincott Williams and Wilkins, Philadelphia, 2006), pp. 1116–1121.
2. K. L. Mohawk, A. R. Melton-Celsa, T. Zangari, E. E. Carroll, A. D. O'Brien, *Microb. Pathog.* **48**, 131 (2010).
3. C. S. Wong, S. Jelacic, R. L. Habeeb, S. L. Watkins, P. I. Tarr, *N. Engl. J. Med.* **342**, 1930 (2000).
4. M. E. Fraser, M. M. Chernaia, Y. V. Kozlov, M. N. James, *Nat. Struct. Biol.* **1**, 59 (1994).
5. S. Mukhopadhyay, C. Bachert, D. R. Smith, A. D. Linstedt, *Mol. Biol. Cell* **21**, 1282 (2010).
6. S. Mukhopadhyay, A. D. Linstedt, *Proc. Natl. Acad. Sci. U.S.A.* **108**, 858 (2011).
7. A. D. Linstedt, A. Mehta, J. Suhan, H. Reggio, H. P. Hauri, *Mol. Biol. Cell* **8**, 1073 (1997).
8. S. Puri, C. Bachert, C. J. Fimmel, A. D. Linstedt, *Traffic* **3**, 641 (2002).
9. R. Natarajan, A. D. Linstedt, *Mol. Biol. Cell* **15**, 4798 (2004).
10. F. Mallard, L. Johannes, *Methods Mol. Med.* **73**, 209 (2003).
11. Materials and methods are available as supporting material on *Science* Online.
12. L. Johannes, D. Tenza, C. Antony, B. Goud, *J. Biol. Chem.* **272**, 19554 (1997).
13. K. Sandvig, B. van Deurs, *Gene Ther.* **12**, 865 (2005).
14. V. Popoff *et al.*, *J. Cell Sci.* **120**, 2022 (2007).
15. F. Mallard *et al.*, *J. Cell Biol.* **143**, 973 (1998).
16. C. Bachert, T. H. Lee, A. D. Linstedt, *Mol. Biol. Cell* **12**, 3152 (2001).
17. M. E. Fraser *et al.*, *J. Biol. Chem.* **279**, 27511 (2004).
18. I. S. Shin *et al.*, *BMB Rep* **42**, 310 (2009).
19. S. Ishikawa *et al.*, *Infect. Immun.* **71**, 3235 (2003).
20. K. L. Mohawk, A. D. O'Brien, *J. Biomed. Biotechnol.* **2011**, 258185 (2011).
21. V. L. Tesh *et al.*, *Infect. Immun.* **61**, 3392 (1993).
22. H. Suzuki, O. Wada, *Environ. Res.* **26**, 521 (1981).
23. J. B. Saenz, T. A. Doggett, D. B. Haslam, *Infect. Immun.* **75**, 4552 (2007).
24. B. Stechmann *et al.*, *Cell* **141**, 231 (2010).
25. S. Fukuda *et al.*, *Nature* **469**, 543 (2011).
26. J. A. Moreno *et al.*, *Toxicol. Sci.* **112**, 394 (2009).
27. M. Aschner, K. M. Erikson, E. Herrero Hernández, R. Tjalkens, *Neuromol. Med.* **11**, 252 (2009).

Acknowledgments: We thank D. R. Smith, T. H. Lee, J. S. Minden, J. L. Brodsky, and M. A. Puthenveedu for advice; N. N. Urban and J. Dry-Henich for help with animal work; Y. Creeger for fluorescence-activated cell sorting; S. Truschel and B. Ballou for protein preparation; and J. Suhan for electron microscopy. Supported by NIH grant R01GM084111 to A.D.L. and an American Heart Association fellowship to S.M. A patent on the use of Mn^{2+} to treat Shiga toxicosis is pending. The data reported in this paper are tabulated in the main text and in the supporting online material.

Supporting Online Material

www.sciencemag.org/cgi/content/full/335/6066/332/DC1
Materials and Methods
Figs. S1 to S17
References (*28*, *29*)

28 October 2011; accepted 5 December 2011
10.1126/science.1215930

Illusions Promote Mating Success in Great Bowerbirds

Laura A. Kelley[1] and John A. Endler[1,2]*

Sexual selection studies normally compare signal strengths, but signal components and sensory processing may interact to create misleading or attention-capturing illusions. Visual illusions can be produced by altering object and scene geometry in ways that trick the viewer when seen from a particular direction. Male great bowerbirds actively maintain size-distance gradients of objects on their bower courts that create forced-perspective illusions for females viewing their displays from within the bower avenue. We show a significant relationship between mating success and the female's view of the gradient; this view explains substantially more variance in mating success than the strength of the gradients. Illusions may be widespread in other animals because males of most species display to females with characteristic orientation and distance, providing excellent conditions for illusions.

Animals produce a vast array of sexual displays (*1*). Signal evolution can be driven by males exploiting sensory biases in females (*2*) but can be limited by psychophysics (*3*), cognitive mechanisms (*4*), and species recognition (*5*). Discussions of signal evolution normally consider only signal intensity (*2*–*5*), but signal components and receiver sensory processes may interact to create misleading or attention-capturing illusions (*6*–*8*) independently of signal strength.

Illusions can arise when the two-dimensional projection of a scene on the retina corresponds to a three-dimensional scene that has geometry different from that of the real scene (*6*). An object viewed by an observer subtends an angle ϕ on the observer's eye, which is dependent on the object's size and distance (Fig. 1 and fig. S1). When objects of similar size increase in distance from an observer, their ϕ values decrease (Fig. 1A, Fig. 2B, and fig. S1A), and this information is unconsciously used to infer the size and distance of objects (*6*, *9*). Forced-perspective illusions occur when the natural relationship between distance and ϕ is violated (*6*–*9*). A scene where objects decrease in size as distance increases (negative gradient) results in more rapidly decreasing ϕ than normal, making the scene appear larger than it is (Fig. 2C), a pattern often found in architecture [see references in (*8*)]. Conversely, a scene where objects increase in size with distance (positive gradient) results in ϕ remaining constant (Figs. 1B and 2A) or decreasing more slowly than normal, and the scene appears smaller (Fig. 2A). Additional illusions may result from object arrangement (*6*) (fig. S2), from interactions between objects and perspective cues (*6*), and when the viewer's head is moved (*7*).

Male bowerbirds construct bowers that serve only to attract females for mating (*10*). Females assess potential mates via various traits, including the number and type of colored decorations (*11*–*13*), vocal mimicry (*14*), and male courtship display movements on the courts (*15*). Male great bowerbirds (*Ptilonorhynchus nuchalis*) construct bowers with an avenue 0.6 m in length, opening onto courts consisting of stones, shells, and bones, collectively called gesso (Fig. 1C), and the male presents colored objects over the gesso during display. Females view males displaying over the court from within the avenue and copulate within the avenue (*10*); this predetermined viewing geometry is an essential requirement for forced perspective (*7*–*9*). Males arrange gesso objects on their display courts so that they increase in size as distance from the bower increases (positive gradient; Fig. 1, B and C), creating forced perspective for the female within the avenue (*8*). Forced perspective could be an honest mate choice signal because males rapidly restore experimentally reversed gradients and vary in their gradient quality (*8*). To investigate whether this illusion influences mate choice, we tested for relationships between mating success and geometry. If the gradients or their generated perspective are important to females, then they should predict the degree of mating success.

We monitored the mating success and court gradients in the population in the eucalyptus woodland at Dreghorn cattle station (20.25°S, 147.73°E) (*8*). The strength of the gradient at each court is the slope (*b*) of the regression of

[1]Centre for Integrative Ecology, School of Life & Environmental Sciences, Deakin University, Geelong, VIC 3216, Australia. [2]School of Marine and Tropical Ecology, James Cook University, Townsville, QLD 4811, Australia.

*To whom correspondence should be addressed. E-mail: john.endler@deakin.edu.au

visual depth (d) or width (w) on distance (x) from the female's viewpoint within the bower avenue (Fig. 1 and fig. S1), and gradient strength is represented by b. All bowers had positive slopes on both courts. The gradient slopes successfully predicted the degree of mating success (Fig. 3A), with visible depth accounting for most of the variation (Table 1).

We measured the perspective view quality according to the standard deviation of the visual angles (s_ϕ) from the female viewpoint; a more regular (even) pattern or texture has a smaller s_ϕ. The regularity of the perspective pattern successfully predicted the degree of mating success (Fig. 3B), with both visible depth and width perspective effects significant (Table 1). The fit to the data is remarkably planar, with an adjusted r^2 of 0.96. This strong linear fit is not an artifact; there are no correlations between the ϕ means and variances (both $P > 0.52$).

The most successful bowers have lower $s_{\phi d}$ and higher $s_{\phi w}$, which suggests that pattern regularity is more important in the vertical (depth) axis than in the horizontal (width) axis. Differential attention to vertical and horizontal axes is known in other animals, including humans (*16*). Bowerbirds may be subject to the horizontal-vertical illusion in which two objects of equal length perpendicular to each other result in the vertical object appearing longer (fig. S2A), as is known in chicks (*6*). The $s_{\phi d}$ and $s_{\phi w}$ coefficients have opposite signs (Table 1), making the prediction plane slant (Fig. 3). This arises because the mean object length/width ratio is 1.4; as the angle to the visual axis of oblong objects increases, ϕ_w increases and ϕ_d decreases. Rough-

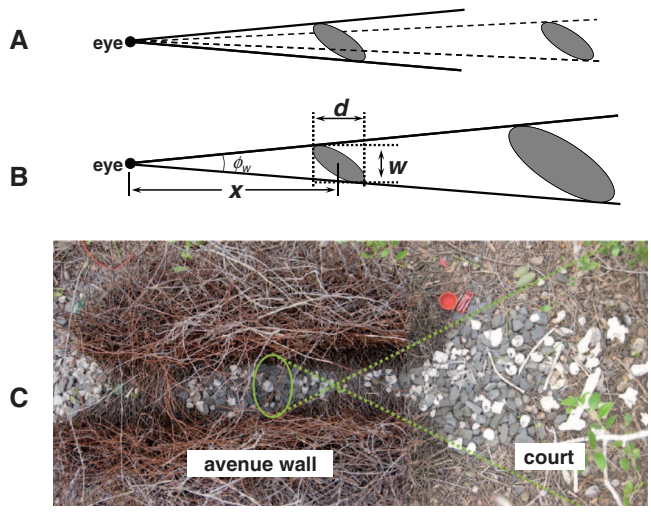

Fig. 1. (**A**) Geometry of normal perspective. Similar-sized objects (ovals) subtend smaller angles (dashed versus solid lines) on the eye (dot) when at greater distances. (**B**) Forced perspective. Larger objects at greater distances subtend the same visual angles if visible width (w) or depth (d) increases with distance (x); ϕ_w is the visible width angle (see fig. S1 for visual depth angle ϕ_d). (**C**) Top view of a bower (only part of left court is shown). Females watch the male display from within the avenue with their head roughly in the center of the avenue (oval), moving their head between the walls (*8*). This leads to a predetermined field of view (dotted lines).

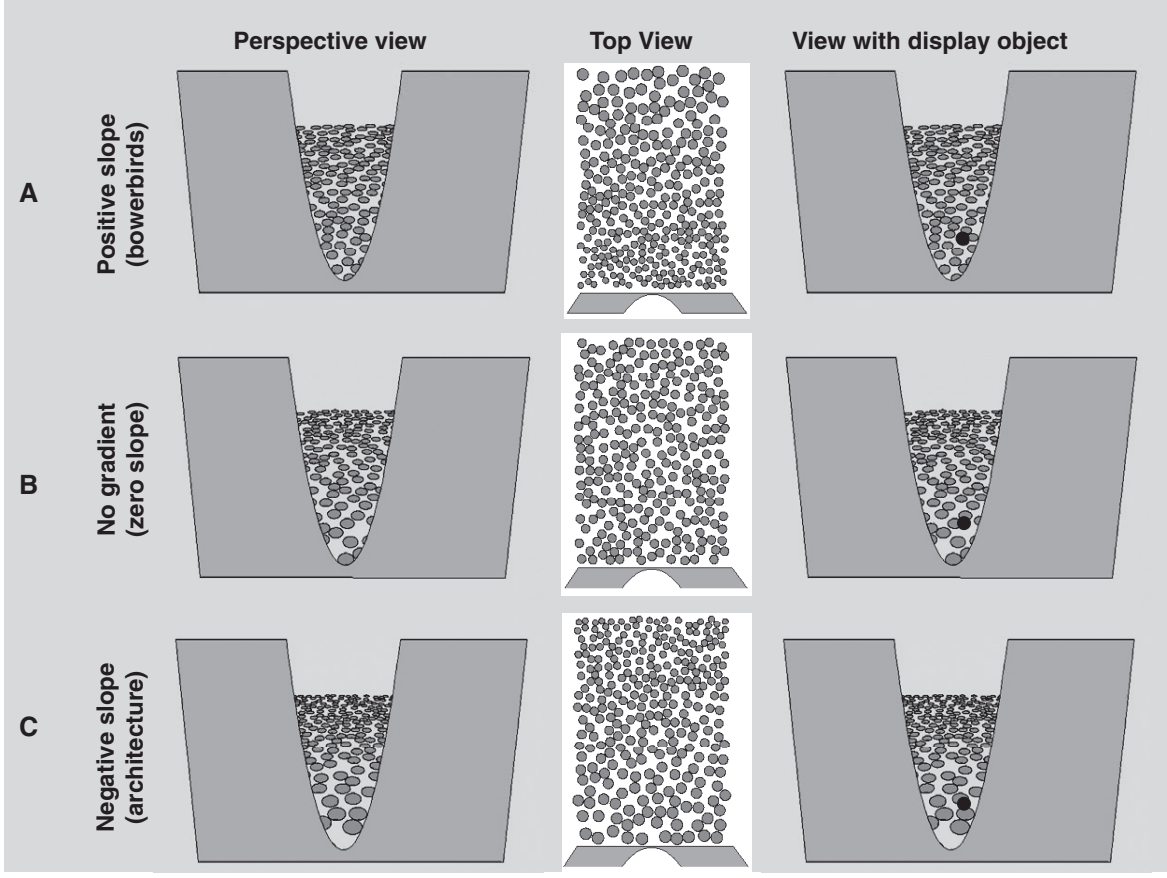

Fig. 2. Three-dimensional scale models of size-distance gradients on a bower court. Left column: Female view of the court from within the avenue (gray area); ovals are court gesso objects. Center column: Court and avenue entrance from above. Right column: Same as left column, with a display object (black) added. Males usually hold display objects at a low point close to the avenue entrance as shown. (**A**) Gesso with a positive size-distance gradient similar to that of a typical great bowerbird court. (**B**) No gradient. (**C**) Negative gradient, as is often found in buildings designed to look large. The positive gradient produces the most regular pattern as seen from the avenue (smallest s_ϕ) and the smallest apparent court size. The Ebbinghaus illusion (fig. S2) makes the display object seem larger in the presence of the positive gradient than in the others, and the magnitude of the effect varies with different slopes (e.g., different males).

ly the same intermediate mating success was achieved with differing combinations of $s_{\phi w}$ and $s_{\phi d}$ (Fig. 3); there are many different ways of producing perspective that can favor the same degree of mating success.

The linear model Akaike information criterion (AIC) values and residuals are much smaller for the perspective view regularity s_ϕ than for the gradient slopes b (Table 1). This indicates that the degree of mating success is more strongly influenced by the perspective view of the court gradients from the female's position within the avenue (measured by s_ϕ) than by the strength of the gradients (b). Therefore, it is the visual effect (illusion) of forced perspective, rather than the gradient slopes, that significantly contributes to mating success.

There are seven possible consequences: (i) The degree of regularity in the perspective view varies among males and could be a mate choice criterion. (ii) The regular visual pattern may make the male's displayed objects more conspicuous; a regular background is less distracting than an irregular one. (iii) Forced perspective may make the court appear smaller than it is (Fig. 2C), possibly causing the display object to appear relatively larger. (iv) Display objects and gesso sizes are similar; 79% (ϕ_w) and 71% (ϕ_d) of the bowers show no mean size difference (Kruskal-Wallace tests, all $P > 0.05$), and the display objects are slightly larger than the gesso in 57% (percentage with positive size difference in ϕ_w) and 79% (ϕ_d) of the bowers. This provides good conditions for the Ebbinghaus illusion (fig. S2B), where an object adjacent to smaller objects will appear larger than the same object next to larger objects (Fig. 2C). This illusion is known in chicks and mistle thrushes, with opposite effects on pigeons (*6*, *17*). It will make display objects vary in apparent size, increasing their conspicuousness. (v) Because display objects are waved toward the female during display, their apparent size may change more rapidly during the display than if the court had normal perspective, and this will be further enhanced by the Ebbinghaus illusion. (vi) The female moves her head within the avenue walls during the male display, providing her with motion parallax depth cues (*7*) that will conflict with the false depth cues of forced perspective. (vii) Motion parallax gives females an estimate of the distance to display objects, yielding a size estimate that will conflict with illusory size estimates generated by forced-perspective and Ebbinghaus illusions.

Any of these seven effects might hold the female's attention longer than if absent, and still longer if the illusions interact. For example, females will not mate unless they have spent more than about 55% of their total time in the avenue watching the male display (fig. S3), and the fraction of avenue time that a female watches a male display is higher for bowers with smaller differences between gesso and display object size ($t = 2.27$, df = 14, $P = 0.039$, $r^2 = 0.27$), as might be expected from the Ebbinghaus illusion. We have direct evidence only for the first effect, but one or more of the other six could also affect mating success. However, we have shown that illusions can affect mating success in ways unpredictable from signal intensity alone.

Our results raise the possibility that illusions may be used by other species during mate choice; sensitivity to visual illusions has been demonstrated in chicks, mistle thrushes, pigeons, and a gray parrot (*6*, *17*–*21*). Mating illusions are a logical extension of the sensory exploitation part of sensory drive (*2*); here, males use sensory biases to mislead or hold attention rather than strongly stimulate. Moreover, the illusion magnitude (*6*) may be a direct-choice criterion. Illusions simply require predictable viewing geometry (*8*); for example, manakins and cock-of-the-rock clear the vicinity of their display courts with characteristic geometry, and in some species females view the male's display from a predictable location and direction (*22*). Even without environmental modification, males of most taxa usually present themselves to females in a particular orientation and move their patterns in particular directions relative to the female visual axis, making illusions possible. Furthermore, given that females in many species prefer males with larger color patches, illusions on the body such as the Ebbinghaus or Wundt-Jastrow (fig. S2) could also be used to alter the apparent size of such patches. This study indicates that illusions could have strong implications for the mode of evolution under sexual selection.

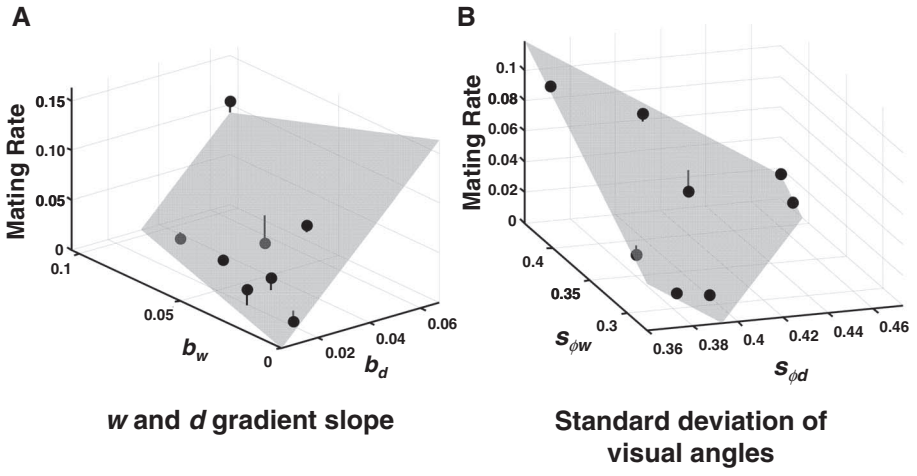

Fig. 3. Mating success predictors. The gray plane is the generalized linear model (*23*) of mating rate on the predictors. Dots are the observed values for each bower; vertical lines are the residuals (most are smaller than the dot size). (**A**) Mating success predicted from the slopes of visual depth and visible width on distance; adjusted $r^2 = 0.725$. (**B**) Mating success predicted by visual angle regularity; adjusted $r^2 = 0.945$.

Table 1. Generalized linear model (*23*) of mating rate (m) on gradient slopes (b_d, b_w) or visual angle standard deviation ($s_{\phi d}$, $s_{\phi w}$) resulting from variation in visible depth d and width w.

Gradient slopes (b) effects, full model $m = b_d + b_w$				Perspective view regularity (s_ϕ) effects, full model $m = s_{\phi d} + s_{\phi w}$			
	β	t (df = 5)	P		β	t (df = 5)	P
Intercept	−0.0162	−1.126	0.31	Intercept	0.210	7.66	0.00061
b_d	2.651	4.06	0.0097	$s_{\phi d}$	−0.912	−10.54	0.00013
b_w	−0.683	−2.031	0.098	$s_{\phi w}$	0.541	9.33	0.00024
Total adjusted $r^2 = 0.725$				Total adjusted $r^2 = 0.945$			
AIC = −37.69 (both b_d and b_w), −34.88 (without b_w), −28.02 (without b_d)				AIC = −50.584 (both $s_{\phi d}$ and $s_{\phi w}$), −29.28 (without $s_{\phi w}$), −27.43 (without $s_{\phi d}$)			

References and Notes

1. M. Andersson, *Sexual Selection* (Princeton Univ. Press, Princeton, NJ, 1994).
2. J. A. Endler, A. L. Basolo, *Trends Ecol. Evol.* **13**, 415 (1998).
3. K. L. Akre, H. E. Farris, A. M. Lea, R. A. Page, M. J. Ryan, *Science* **333**, 751 (2011).
4. M. Bateson, S. D. Healy, *Trends Ecol. Evol.* **20**, 659 (2005).
5. S. R. Pryke, M. Andersson, *Behav. Ecol.* **19**, 1116 (2008).
6. S. Coren, J. S. Girgus, *Seeing Is Deceiving: The Psychology of Visual Illusions* (Erlbaum, Hillsdale, NJ, 1978).
7. B. Rogers, A. Gyani, *Perception* **39**, 330 (2010).
8. J. A. Endler, L. C. Endler, N. R. Doerr, *Curr. Biol.* **20**, 1679 (2010).
9. H. E. Ross, C. Plug, in *Perceptual Constancy, Why Things Look as They Do*, V. Walsh, J. Kulikowski, Eds. (Cambridge Univ. Press, Cambridge, 1998), pp. 499–528.
10. C. B. Frith, D. W. Frith, *The Bowerbirds* (Oxford Univ. Press, Oxford, 2004).
11. J. R. Madden, *Behav. Ecol. Sociobiol.* **53**, 263 (2003).
12. G. Borgia, *Anim. Behav.* **33**, 266 (1985).
13. J. A. Endler, D. A. Westcott, J. R. Madden, T. Robson, *Evolution* **50**, 1795 (2005).
14. S. W. Coleman, G. L. Patricelli, B. Coyle, J. Siani, G. Borgia, *Biol. Lett.* **3**, 463 (2007).

15. G. L. Patricelli, J. A. C. Uy, G. Walsh, G. Borgia, *Nature* **415**, 279 (2002).
16. S. C. Dakin, R. J. Watt, *J. Vis.* **9**, 2.1 (2009).
17. N. Nakamura, S. Watanabe, K. Fujita, *J. Exp. Psychol.* **34**, 375 (2008).
18. N. Nakamura, K. Fujita, T. Ushitani, H. Miyata, *J. Comp. Psychol.* **120**, 252 (2006).
19. S. Watanabe, N. Nakamura, K. Fujita, *Cognition* **119**, 137 (2011).
20. K. Fujita, D. S. Blough, P. M. Blough, *Anim. Learn. Behav.* **19**, 283 (1991).
21. I. M. Pepperberg, J. Vicinay, P. Cavanagh, *Perception* **37**, 765 (2008).
22. J. A. Endler, M. Théry, *Am. Nat.* **148**, 421 (1996).
23. R Development Core Team, *R: A Language and Environment for Statistical Computing* (R Foundation for Statistical Computing, Vienna, 2011; www.R-project.org).

Acknowledgments: We thank the Smith family for access and hospitality at Dreghorn Station; L. Endler for help in fieldwork and photograph analysis; Deakin University for financial support; and L. Barrett, B. Buttemer, J. Madden, S. Nakagawa, M. Richardson, J. Zeil, and two anonymous reviewers for excellent comments on the manuscript. The field research was done with an EPA-Queensland Parks and Wildlife Service permit (WISP01994004) and ethics approval from Deakin University (A22-2010) and James Cook University (A1318). Data are in the supporting online material.

Supporting Online Material
www.sciencemag.org/cgi/content/full/335/6066/335/DC1
Materials and Methods
Figs. S1 to S3
Tables S1 to S4
Movies S1 and S2

9 August 2011; accepted 22 November 2011
10.1126/science.1212443

Activation-Induced B Cell Fates Are Selected by Intracellular Stochastic Competition

Ken R. Duffy,[1] Cameron J. Wellard,[2,3] John F. Markham,[4] Jie H. S. Zhou,[2,3] Ross Holmberg,[2] Edwin D. Hawkins,[5] Jhagvaral Hasbold,[2,3] Mark R. Dowling,[2,3]*† Philip D. Hodgkin[2,3]*†

In response to stimulation, B lymphocytes pursue a large number of distinct fates important for immune regulation. Whether each cell's fate is determined by external direction, internal stochastic processes, or directed asymmetric division is unknown. Measurement of times to isotype switch, to develop into a plasmablast, and to divide or to die for thousands of cells indicated that each fate is pursued autonomously and stochastically. As a consequence of competition between these processes, censorship of alternative outcomes predicts intricate correlations that are observed in the data. Stochastic competition can explain how the allocation of a proportion of B cells to each cell fate is achieved. The B cell may exemplify how other complex cell differentiation systems are controlled.

Production of antibody by B cell–derived plasma cells is critical for an effective immune response (*1*), but B cell activation mechanisms leading to the formation of plasma cells are numerous and poorly understood. One known mechanism is for the B cell to use its surface receptor to capture and internalize antigen, which leads to presentation of T cell epitopes on its cell surface (*2*). Upon detection, a T cell delivers cell contact– and cytokine-mediated signals (*3*) that lead to B cell proliferation or changes in antibody type (isotype switching) (*4*), as well as differentiation into dividing plasmablasts (PBs) and sessile, long-lived plasma cells, both of which secrete antibody (*5*, *6*). The heterogeneous B cell fates resulting from isotype switching and development into PBs can be replicated in vitro by stimulating naïve B cells through CD40 in addition to the cytokines interleukin 4 (IL-4) and IL-5 to simulate T cell interaction (*7*, *8*), a method we used. As Blimp1 is a transcription factor that is selectively required for differentiation to PB, we used a Blimp1-GFP reporter mouse (*9*) to identify PBs by green fluorescent protein (GFP) expression and fluorescently labeled antibody against immunoglobulin G1 (IgG1) to identify cells switched to IgG1. After an initial 3-day culture, single-cell video microscopy was used to observe sorted cells from generations 1, 3, 5, and 7 that do not express Blimp1 or IgG1 and to optically track their times to isotype switch to IgG1, to differentiate to PBs, and ultimately to division or death (Fig. 1A and fig. S1) (*10*). Only one division round was followed because of the strong homotypic adhesion of B lymphoblasts, which leads to a loss of identity.

As found previously (*11*–*15*), division and death times were highly variable, and this was also true for times to isotype switching and commitment to become a PB (Fig. 1, B and C). Consistent with earlier population studies (*11*, *16*), the dependence of frequency of isotype switching, as well as other parameters, on generation is apparent (Fig. 1, D and E). Despite the diverse range of experience of individual cells, the population-level response is insensitive to this variability (*12*, *13*, *17*–*20*), which presents the conundrum of how to reconcile the single-cell and population-level responses. Furthermore, these data have complex correlation structures, both within single cells (intracellular) and between siblings (intercellular), which pose an additional challenge to any paradigm of understanding.

As a representative of intracellular correlation, for all cells that differentiate and go on to divide, Fig. 2A presents a scatter plot of times to these events, as well as estimates of Pearson's correlation coefficient (ρ). The latter reveals positive correlation coefficients for cells of each generation (ρ: 0.54, 0.59, 0.56, and 0.80). Analysis of other combinations shows that time to differentiate to PBs is positively correlated with time to death (fig. S2A) (ρ: 0.70, 0.54, 0.81, and 0.54), and with time to isotype switch (Fig. 2C) (ρ: –, 0.34, 0.29, and 0.51), where a dash indicates an insufficient number of observations to form an estimate. There is little evidence for correlation in time to isotype switch and time to division (Fig. 2B) (ρ: –, 0.17, −0.05, and −0.08) or death (fig. S2B) (ρ: –, 0.15, 0.08, and 0.11).

For intercellular dependencies, we can investigate the existence of concordance in sibling fates. Visual inspection of Fig. 1B suggests strong positive relatedness between siblings. To quantify the strength of concordance in opposing fates of siblings, we use Yule's Q (*21*). It takes a value in [−1, 1], with 1 corresponding to perfect positive correlation, and 0 corresponding to no correlation in sibling fate (*10*). For our system, the opposing fates of siblings are death versus division, differentiation to PBs versus no differentiation to PBs, and isotype switching versus no isotype switching. Figure 2D plots Yule's Q for the division versus death outcome of siblings. It is high for all generations (Q: 0.97, 0.93, 0.90, and 0.96), which confirms strong sibling concordance in division or death fates: If a cell dies or divides, the likelihood that its sibling experiences the same fate is substantially higher than the likelihood of a cell chosen uniformly at random from the population at large has the same fate. All other fates display similar evidence of strong concordance: differentiate to PB versus not (Fig. 2E) (Q: 0.98, 0.98, 0.92, and 0.93) and isotype switch versus not (Fig. 2E) (Q: –, 0.98, 0.99, and 0.94).

This strong concordance justifies investigating correlations within the times to fates of siblings. We found strong correlation in time to fate between siblings (Fig. 2, F and G): ρ of 0.90, 0.93, 0.84, and 0.82 for division and ρ of 0.85, 0.79, 0.72, and 0.77 for death. For differentiation

[1]Hamilton Institute, National University of Ireland, Maynooth, Ireland. [2]Walter and Eliza Hall Institute of Medical Research, Parkville, Melbourne, Victoria 3052, Australia. [3]Department of Medical Biology, University of Melbourne, Melbourne, Victoria 3052, Australia. [4]Victoria Research Laboratory, National Information and Communications Technology (ICT) Australia, University of Melbourne, Melbourne, Victoria 3010, Australia. [5]Immune Signalling Laboratory, Peter MacCallum Cancer Centre, Melbourne, Victoria 3002, Australia.

*These authors contributed equally to this work.
†To whom correspondence should be addressed. E-mail: hodgkin@wehi.edu.au